

Article

Inhibition of aryl hydrocarbon receptor signaling promotes the terminal differentiation of human erythroblasts

Yijin Chen ¹, Yong Dong¹, Xulin Lu², Wanjing Li¹, Yimeng Zhang¹, Bin Mao¹, Xu Pan¹, Xiaohong Li¹, Ya Zhou¹, Quanming An¹, Fangxin Xie¹, Shihui Wang³, Yuan Xue¹, Xiping Cai¹, Mowen Lai¹, Qiongxiu Zhou¹, Yan Yan⁴, Ruohan Fu⁴, Hong Wang¹, Tatsutoshi Nakahata⁵, Xiuli An⁶, Lihong Shi², Yonggang Zhang^{1,*}, and Feng Ma^{1,2,*}

¹ Institute of Blood Transfusion, Chinese Academy of Medical Sciences & Peking Union Medical College (CAMS & PUMC), Chengdu 610052, China

² State Key Laboratory of Experimental Hematology, Institute of Hematology and Blood Diseases Hospital, CAMS & PUMC, Tianjin 300020, China

³ School of Life Sciences, Zhengzhou University, Zhengzhou 450001, China

⁴ Department of Obstetrics and Gynecology, Jinjiang Maternity and Child Health Hospital, Chengdu 610065, China

⁵ Center for iPS Cell Research and Application (CiRA), Kyoto University, Kyoto 606-8507, Japan

⁶ Laboratory of Membrane Biology, New York Blood Center, New York, NY 10065, USA

* Correspondence to: Yonggang Zhang, E-mail: yonggangzhang@ibt.pumc.edu.cn; Feng Ma, E-mail: mafeng@ibt.pumc.edu.cn

Edited by Anming Meng

The aryl hydrocarbon receptor (AHR) plays an important role during mammalian embryo development. Inhibition of AHR signaling promotes the development of hematopoietic stem/progenitor cells. AHR also regulates the functional maturation of blood cells, such as T cells and megakaryocytes. However, little is known about the role of AHR modulation during the development of erythroid cells. In this study, we used the AHR antagonist StemRegenin 1 (SR1) and the AHR agonist 2,3,7,8-tetrachlorodibenzo-*p*-dioxin during different stages of human erythropoiesis to elucidate the function of AHR. We found that antagonizing AHR signaling improved the production of human embryonic stem cell derived erythrocytes and enhanced erythroid terminal differentiation. RNA sequencing showed that SR1 treatment of proerythroblasts upregulated the expression of erythrocyte differentiation-related genes and downregulated actin organization-associated genes. We found that SR1 accelerated F-actin remodeling in terminally differentiated erythrocytes, favoring their maturation of the cytoskeleton and enucleation. We demonstrated that the effects of AHR inhibition on erythroid maturation were associated with F-actin remodeling. Our findings help uncover the mechanism for AHR-mediated human erythroid cell differentiation. We also provide a new approach toward the large-scale production of functionally mature human pluripotent stem cell-derived erythrocytes for use in translational applications.

Keywords: erythroblast, AHR, SR-1, human pluripotent stem cells, differentiation

Introduction

The aryl hydrocarbon receptor (AHR) is a member of the basic-helix–loop–helix Per–ARNT–SIM family of transcription factors, which play important roles in various physiological processes (Nebert, 2017). AHR can be activated by endogenous or exogenous ligands and is involved in the regulation of inflam-

mation (Juricek et al., 2017; Neavin et al., 2018; Guarnieri et al., 2020), cell differentiation (Mascanfroni et al., 2015; Furue et al., 2018), apoptosis (Shinde et al., 2018), cancer progression (Murray et al., 2014), and neural function (Juricek and Coumoul, 2018). Several studies indicate that AHR has an essential role in hematopoiesis (Boitano et al., 2010; Lindsey and Papoutsakis, 2012; Angelos et al., 2017, 2018; Leung et al., 2018). AHR^{-/-} mice show a marked increase in the number of hematopoietic stem cells (HSCs) in the bone marrow and an increased propensity to develop lymphomas (Singh et al., 2011; Unnisa et al., 2016; Bennett et al., 2018). Cultures of human pluripotent stem cells (hPSCs), either those treated with the AHR antagonist StemRegenin 1 (SR1) or those in which the

Received November 3, 2021. Accepted November 6, 2021.

© The Author(s) (2022). Published by Oxford University Press on behalf of *Journal of Molecular Cell Biology*, CEMCS, CAS.

This is an Open Access article distributed under the terms of the Creative Commons Attribution-NonCommercial License (<https://creativecommons.org/licenses/by-nc/4.0/>), which permits non-commercial re-use, distribution, and reproduction in any medium, provided the original work is properly cited. For commercial re-use, please contact journals.permissions@oup.com

AHR gene was deleted, have increased levels of CD34⁺CD45⁺ hematopoietic stem/progenitor cells (HSPCs); there was also a significant increase in the number of colony-forming-unit erythrocytes (CFU-Es) and colony-forming-unit macrophages (CFU-Ms) (Angelos et al., 2017). Moreover, recent research shows that AHR is involved in the determination of cell fate. Activation of AHR promotes cellular differentiation toward the formation of monocyte-derived dendritic cells by inhibiting the formation of macrophages (Goudot et al., 2017). Furthermore, AHR plays an important role in the differentiation of B cells (Sherr and Monti, 2013; Li et al., 2017a), natural killer cells (Scoville et al., 2018), and megakaryocytes (Lindsey and Papoutsakis, 2011; Strassel et al., 2016).

Following commitment to the erythroid lineage, HSCs sequentially give rise to common myeloid progenitor, megakaryocyte-erythrocyte progenitor (MEP), burst-forming-unit erythroid (BFU-E), and CFU-E cells (Li et al., 2014). Subsequently, erythroid progenitors enter terminal differentiation, sequentially produce morphologically recognizable proerythroblasts, basophilic, polychromatic, and orthochromatic erythroblasts, and reticulocytes, and finally mature into red blood cells. During maturation, erythroblasts undergo serial changes, during which the cell and the nucleus decrease in size, hemoglobin is synthesized, membrane proteins are reorganized, chromatin condensation is regulated, and finally, cells become enucleated (Hattangadi et al., 2011; An et al., 2014). The expression of AHR is upregulated in HSCs and MEP cells, but gradually downregulated during erythroid differentiation (Smith et al., 2013). This finding suggests that the differential modulation of AHR is important during the process of erythropoiesis. In MEP cells, chronic AHR activation causes differentiation of erythroid cells, and repression of AHR activity leads to megakaryocyte specification (Smith et al., 2013). However, several reports show that exposure of zebrafish (Belair et al., 2001; Carney et al., 2006) and human (Sakamoto et al., 2004) erythrocytes to the AHR agonist 2,3,7,8-tetrachlorodibenzo-*p*-dioxin (TCDD) damaged the deformation ability of erythrocytes and decreased hemoglobin synthesis. Thus, the role of AHR in the development and differentiation of erythroid cells is still ambiguous.

Remodeling of F-actin is essential for nuclear extrusion during the terminal differentiation of erythroid cells (Nigra et al., 2020). The expression of actin reaches a peak in proerythroblasts, and F-actin forms a ring structure underneath the cytoplasmic membrane. During terminal differentiation, F-actin rearranges and forms a contractile ring between the extruding nucleus and the incipient reticulocyte, which benefits erythroblast enucleation (Li et al., 2017b; Uras et al., 2017; Ubukawa et al., 2020). F-actin remodeling is regulated by many factors, including AHR, which regulates the expression of actin-related genes to modulate cellular shape and function (Carvajal-Gonzalez et al., 2009; Reyes-Hernandez et al., 2009; Murai et al., 2018; Merches et al., 2020). AHR activation by TCDD impairs the deformation ability of erythroid cells, indicating that AHR may have a role in the development of the erythroid cytoskeleton.

In this study, by an efficient co-culture system we established to induce hematopoietic and erythroid differentiation from hPSCs (Ma et al., 2008; Mao et al., 2016; Zhou et al., 2019), we used the AHR antagonist SR1 to show that inhibiting AHR signaling promotes erythroid terminal differentiation. Particularly, SR1 promotes actin to be localized to one side of the cell near the nucleus, showing that AHR signaling relates to cytoskeletal remodeling during erythroid terminal differentiation. Furthermore, addition of SR1 to cultures of human embryonic stem cell (hESC)-derived erythroid cells during terminal differentiation increases the number of enucleated erythrocytes that can be harvested. These findings increase our knowledge of AHR's function during erythroid differentiation, and provide a possible way to enhance the production and maturation of hESC-derived mature erythrocytes.

Results

SR1 increases erythroid cell production from hESC

We have described previously an efficient system of producing HSPC from hESC by co-culturing with aorta-gonad-mesonephros (AGM)-S3 (Mao et al., 2016; Zhou et al., 2019; Dong et al., 2020). In this system, hematopoietic endothelial cells (HECs; CD34⁺KDR⁺CD43⁻GPA⁻) and hematopoietic progenitor cells (HPCs; CD34⁺CD43⁺CD45⁻GPA⁻) can be detected on co-culture day 6 (co-D6) and co-D10 (Zhou et al., 2019). In addition, HSPCs (CD34⁺CD45⁺) emerge at co-D10 and reach a peak at co-D14. Early erythroblasts (CD34⁺GPA⁺) can also be observed before the emergence of HSPCs (Mao et al., 2016).

In the current study, SR1 was continuously added to the co-culture system from co-D6, and total cells were harvested every 2 days until co-D14 for fluorescence-activated cell sorting analysis (Figure 1A). As previously reported (Angelos et al., 2017), SR1 treatment significantly increased the number of HPCs and HSPCs compared with the dimethyl sulfoxide (DMSO) treated control (Figure 1B and C). Besides, SR1-mediated enhancement of HSPC production was accompanied by an increase in the number of erythroid (CD71⁺GPA⁺) and myeloid (CD45⁺GPA⁻CD34⁻) cells. Of note, SR1 significantly increased the number of early erythroblasts but not the number of myeloid cells at co-D8, when HSPCs have not emerged. Under TCDD condition, the production of HPCs and myeloid cells was markedly decreased, but a similar decrease was not observed in the production of HSPCs as compared with the DMSO control. In addition, there was a significant reduction in production of erythroid cells at co-D14 in TCDD-treated cells (Figure 1C). These data indicate that inhibited AHR may have a role in erythropoiesis.

To investigate whether inhibited AHR can influence the development of hESC-derived early erythroblasts, sorted co-D6 HECs were exposed to SR1 for 3 days and used in the colony-forming-unit assay. More HPCs were generated from co-D6 HECs, but there was no significant difference in HEC-derived CFU-E colonies between SR1- and DMSO-treated cells (Supplementary Figure S1A–C). More colonies were produced from SR1-treated HPCs, including granulocytic-erythroid-megakaryocytic-macrophagic (GEMM), BFU-E, and granulocyte or macrophage

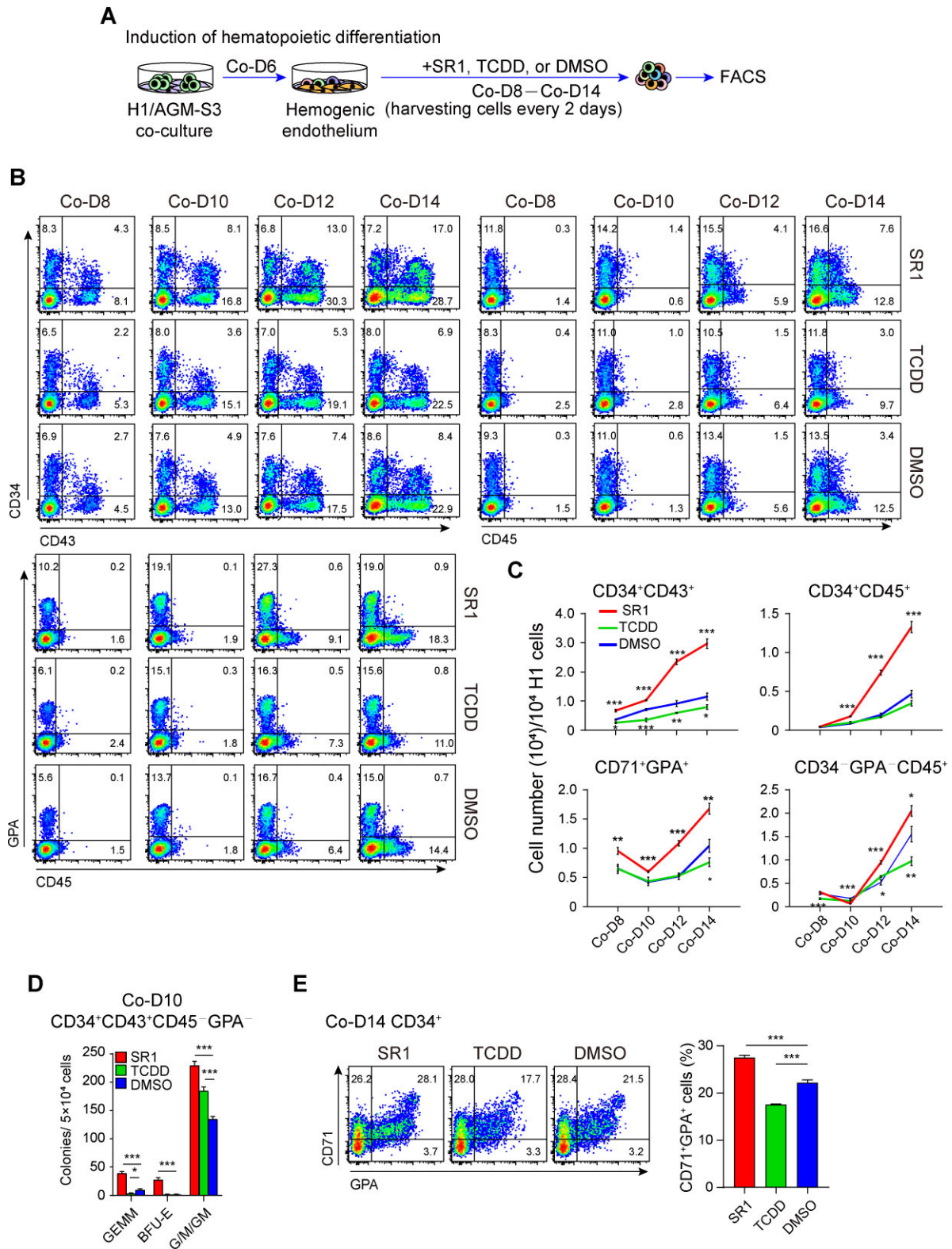


Figure 1 SR1 increases erythroid cell production from hESCs. **(A)** A schematic of the strategy used to analyze the effect of SR1 on hematopoiesis. SR1 was continuously added from D6 onward during H1/AGM-S3 co-culture (co-D6), and total cells were harvested every 2 days for flow cytometry analysis and the colony-forming-unit assay. DMSO was added as the vehicle control. **(B and C)** Flow cytometry analysis **(B)** and absolute cell number **(C)** of hematopoietic cells (CD34⁺CD43⁺), HSPCs (CD34⁺CD45⁺), erythroid cells (CD71⁺GPA⁺), and

or granulocyte/macrophage (G/M/GM) colonies compared with DMSO treatment, while fewer GEMM colonies were generated from TCDD-treated HPCs (Figure 1D). A higher percentage of CD71⁺GPA⁺ cells were detected in SR1-treated co-D14 CD34⁺ cells compared with the DMSO-treated control at D3, while TCDD-treated cultures showed opposite results (Figure 1E). Similar results were observed in umbilical cord blood (UCB)-derived CD34⁺ cells (Supplementary Figure S1D). Although chronic SR1 treatment generated fewer cells, the percentage of erythroid cells was always higher in SR1-treated cultures than in DMSO-treated cultures (Supplementary Figure S1D and E). Collectively, these data suggest that AHR antagonism has a positive effect on erythroid differentiation rather than generation from hematopoietic progenitors.

AHR antagonism promotes erythroid terminal differentiation

We wondered whether AHR inhibition increases CD71⁺GPA⁺ cells and CFU-E colonies by acting on BFU-E cells. To test this hypothesis, UCB-derived BFU-E cells isolated by the expression of the surface marker CD34⁺CD71⁺GPA⁻CD123⁻ (Li et al., 2014) at D4 were continuously exposed to SR1 or DMSO. More GPA⁺ erythroid cells were produced at D2 and D3 with more CFU-E colony-forming ability under SR1 condition (Figure 2A–C). However, the percentage of GPA⁺ cells was much higher at D6, but the number of these cells was lower in SR1-treated cells than in the control (Figure 2A and B), which was coincident with chronic SR1-treated CD34⁺ cells at D6 and D8 (Supplementary Figure S1E). These results suggest that AHR antagonism may have a role in erythroid terminal differentiation.

To further assess the role of AHR during erythroid terminal differentiation, D7 CFU-E-enriched cells (CD71⁺GPA⁻) (Ludwig et al., 2019) and proerythroblasts (CD71⁺GPA^{low}) were continuously exposed to SR1, TCDD, or DMSO. Results showed that more GPA⁺ cells were generated from cultures of CD71⁺GPA⁻ cells (Figure 2D), and the expression of GPA was higher in proerythroblasts (Figure 2E) under SR1 condition at D3. TCDD significantly inhibited these processes. In addition, there was no significant difference in the level of apoptosis in cells derived from SR1-, TCDD-, or DMSO-treated CD71⁺GPA⁻ cells or proerythroblasts (Supplementary Figure S2A and B). The result of cell cycle indicated that fewer cells in S phase but more in G0/G1 phase were observed in both SR1- and TCDD-treated cells (Supplementary Figure S2C and D). SR1-treated CD71⁺GPA⁻ cells and proerythroblasts showed smaller cell size and lighter basophilic cytoplasm, whereas TCDD-treated cells showed the opposite results (Figure 2F). Furthermore, proteomic analysis showed that the expression of skeleton proteins (tropomyosin 3, spectrin, adducin, and ankyrin), membrane proteins (CD44,

CD47, 4.1R, stomatin, and MPP1), and globins (α -globin and β -globin) was higher in SR1-treated proerythroblasts than in DMSO-treated proerythroblasts (Figure 2G). The flow cytometry results also showed higher expression of β -globin, CD44, and CD47 in SR1-treated cells (Figure 2H). To test whether other agonists or antagonists of AHR had similar effects on erythroid terminal differentiation, UCB-derived proerythroblasts were exposed to 2-(1'*H*-indole-3'-carbonyl)thiazole-4-carboxylic acid methyl ester (ITE, an endogenous agonist), 6-formylindolo[3,2-*b*]-carbazole (FICZ, an endogenous agonist), or *N*-(2-(1'*H*-indol-3-yl)ethyl)-9-isopropyl-2-(5-methylpyridin-3-yl)-9*H*-purin-6-amine (GNF351, an antagonist) for 3 days. GNF351 promoted terminal differentiation, but ITE and FICZ inhibited terminal differentiation (Supplementary Figure S2E).

Next, we wondered whether AHR had similar effects on H1-derived erythroid cells. Co-D14 CD34⁺ cell-derived CD71⁺GPA⁻ cells and proerythroblasts were sorted at D7 of erythroid differentiation. Similar trends to those seen in UCB-derived cells were observed in H1-derived cells (Supplementary Figure S3A–C). Moreover, the production of CFU-E colonies was higher in both SR1-treated CD71⁺GPA⁻ cells and proerythroblasts than in DMSO-treated cells (Supplementary Figure S3D). In addition, SR1 enhanced the differentiation of H1-derived early erythroblasts and the ability to form CFU-E colonies (Supplementary Figure S3E and F). Taken together, these results demonstrate that AHR inhibition promotes the terminal differentiation of human erythroid cells, whereas AHR activation arrests this process.

Inhibition of AHR influences heme- and actin-related gene expression during terminal erythroid differentiation

To determine the cellular processes by which AHR antagonism enhances terminal differentiation, H1 hESC (H1)- or UCB-derived proerythroblasts treated for 3 days with SR1 were collected for RNA sequencing (RNA-seq) analysis. SR1 treatment of UCB-derived cells upregulated the expression of 460 out of 1282 genes and downregulated the expression of 822 genes (Figure 3A). Similar patterns were observed in H1-derived cells (expression of 1365 genes was upregulated and expression of 1736 genes was downregulated). The expression of AHR-regulated genes such as cytochrome P450 family 1 subfamily B member 1 (*CYP1B1*) and *AHRR* was markedly downregulated in SR1-treated cells (Supplementary Figure S4A). To find upregulated and downregulated genes common to SR1-treated H1- and UCB-derived erythroid cells, we overlapped transcriptomic profiles from these two cell types. We found that the expression of 162 upregulated and 440 downregulated genes was common to both cell types. Next, gene ontology enrichment (EGO) analysis was performed on these genes.

Figure 1 (Continued) myeloid cells (CD34⁻GPA⁻CD45⁺) treated with or without SR1 from co-D8 to co-D14. (D) Isolated co-D10 hematopoietic progenitor cells (CD34⁺CD43⁺CD45⁻GPA⁻) were replanted on AGM-S3 including hematopoietic differentiation medium, and the clonogenic capacity of these cells treated with or without SR1 at D3 was measured. The numbers of GEMM, BFU-E, CFU-E, and G/M/GM colonies are shown. (E) Co-D14-derived CD34⁺ cells were cultured in erythroid differentiation medium, and the proportion of CD71⁺GPA⁺ cells was analyzed by flow cytometry at D3. All values are mean \pm SD, $n = 3$; * $P < 0.05$, ** $P < 0.01$, *** $P < 0.001$.

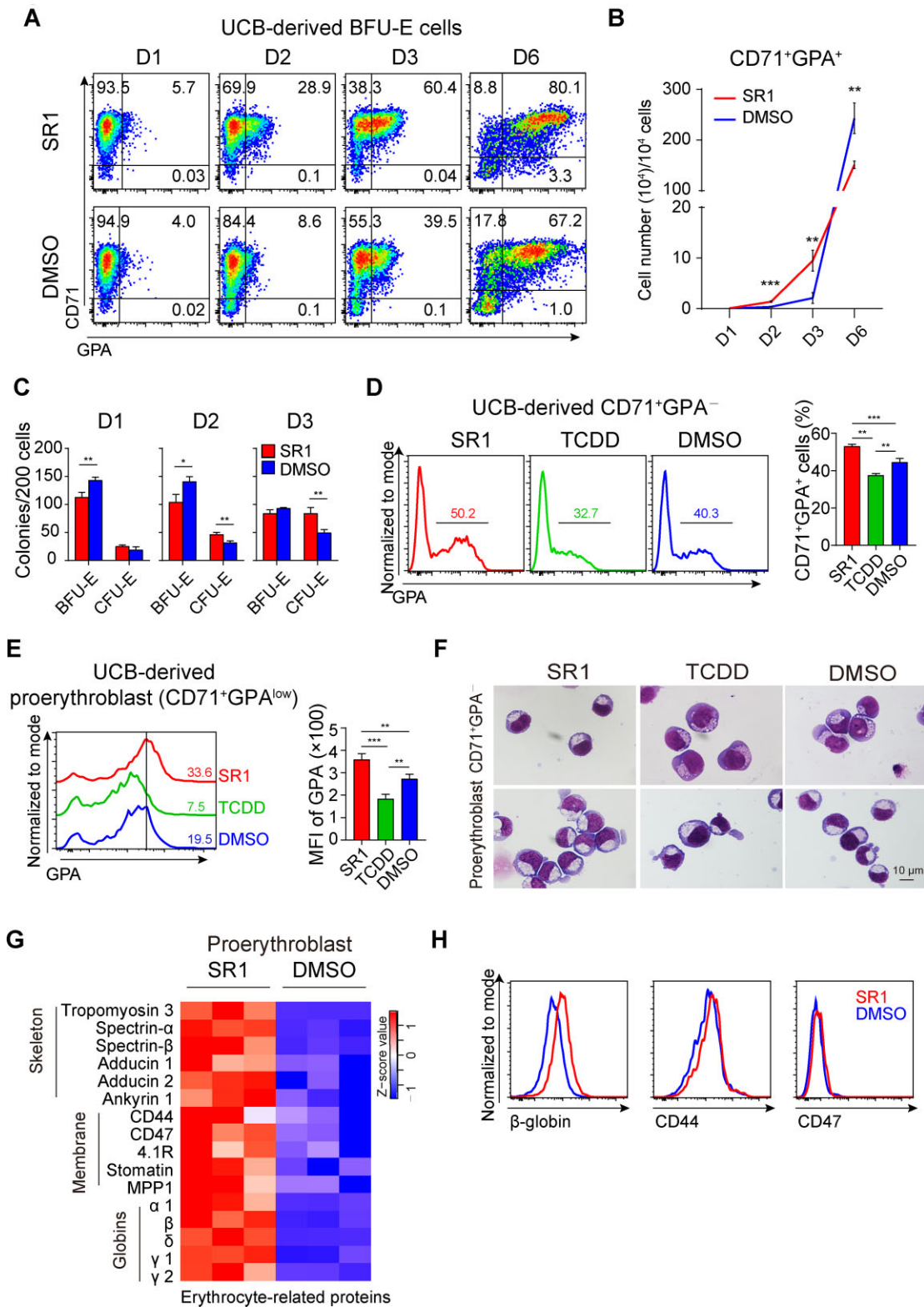


Figure 2 AHR antagonism promotes erythroid terminal differentiation. **(A and B)** Sorted UCB-derived BFU-E cells were treated continuously with or without SR1, and the proportion of CD71⁺GPA⁺ cells was analyzed by flow cytometry **(A)** and the number of these cells was calculated at D1, D2, D3, and D6 by the colony-forming-unit assay **(B)**. **(C)** The number of BFU-E and CFU-E colonies at D1, D2, and D3. **(D and E)** Isolated CFU-E-enriched cells (CD71⁺GPA⁻) and proerythroblasts (CD71⁺GPA^{low}) were treated with SR1, TCDD, or DMSO. **(D)** Flow cytometry analysis

Results showed that upregulated genes were highly associated with erythroid differentiation and homeostasis, as well as heme metabolic processes (Figure 3B). Genes involved in the erythroid differentiation processes were hemoglobin synthesis-related genes (*AHSP*, *ALAS2*, *TMEM14C*, and *SOX6*), membrane protein-related genes (*SLC4A1* and *EPB42*), and erythropoietin signal-related genes (*JAK2* and *MFHAS1*) (Supplementary Figure S4B). In addition, 440 SR1-downregulated genes were enriched in actin-related processes, such as actin filament organization and regulation of small GTPase-mediated signal transduction (Figure 3C). Furthermore, gene set enrichment analysis (GSEA) showed that SR1 treatment downregulated several actin cytoskeleton-associated genes (Figure 3D; Supplementary Figure S4C). Together, these data show that AHR inhibition upregulates the expression of erythroid differentiation- and heme metabolism-related genes, whereas it downregulates the expression of actin-associated genes.

To further confirm the result, SR1- or DMSO-treated proerythroblasts (CD71⁺GPA^{low}) and CD71⁺GPA^{high} cells were sorted for RNA-seq analysis, respectively. The genes associated with erythrocyte differentiation and oxygen transport were upregulated, and those related to actin filament organization were downregulated in SR1-treated CD71⁺GPA^{high} cells (Figure 3D and E). Although EGO analysis did not show erythroid-related items in SR1-treated proerythroblasts, the expression of *HBB*, *HBD*, *SCL4A1*, and *MFHAS1* was upregulated in SR1-treated cells (Figure 3F). Besides, the expression of actin-related genes (like *MYO1G*, *MYO19*, and *ACTG1*) was downregulated by SR1 treatment (Figure 3G).

Together, these serial findings show that AHR inhibition promotes terminal erythroid differentiation and suggest that AHR may relate to the actin cytoskeleton during this process.

Disrupting F-actin assembly can block the function of AHR antagonists on erythroid terminal differentiation

Next, we examined actin expression during SR1 treatment. RNA-seq results showed that *ACTB* (β -actin) expression was decreased in SR1-treated proerythroblasts (Figure 4A). Western blotting results showed that SR1 treatment decreased β -actin expression in proerythroblasts (Figure 4B). Phalloidin was used as a marker of F-actin expression. We found that the amount of F-actin gradually decreased during the differentiation of proerythroblasts. Moreover, cells with lower F-actin expression had actin rearrangement at D3 (red arrow; Figure 4C), and polarized F-actin was formed, which localized at one side of the nucleus at D5 (white arrow; Figure 4C). There was a significant increase in F-actin remodeling at D3, and actin polarization was more obvious

on D5 in SR1-treated cells, while TCDD prevented F-actin remodeling and actin polarization (Figure 4C). To further examine the correlation between AHR and actin remodeling, two actin-disrupting drugs, cytochalasin-D (CytoD) and jasplakinolide, were used. Surprisingly, CytoD, which blocks polymerization and elongation of F-actin, did not influence the differentiation of proerythroblasts but reversed the action of SR1 on these cells (Figure 4D). Jasplakinolide, which stabilizes F-actin, produced similar results on SR1-treated proerythroblasts (Figure 4E). Similar results to those produced by CytoD, which reversed the effect of SR1 on proerythroblast differentiation, were observed in GNF351-treated UCB-derived cells (Figure 4F) and SR1-treated H1-derived proerythroblasts (Figure 4G). These data confirmed that AHR antagonism can accelerate F-actin remodeling and that disrupting F-actin remodeling blocks the promoting effect of AHR antagonism on erythroid terminal differentiation.

SR1 benefits the functional maturation of human erythroid cells

Since SR1 promotes terminal erythroid differentiation, we assessed whether SR1 modulated the maturation of human erythroid cells. Co-D14 or UCB-derived CD34⁺ cells were collected and recultured in erythroid differentiation medium; SR1 was added at D7 (Figure 5A). First, we examined the expression of erythroid-related proteins on co-D14-derived erythroid cells at D12. Under SR1 conditions, the expression of Band3, CD47, and β -globin was higher, but CD49d expression was lower (Supplementary Figure S5A and B). However, the expression of CD29 and CD44 did not change (Supplementary Figure S5A). At D21, the concentration of hemoglobin was higher in SR1-treated erythroid cells (45 g per 10¹² cells) than in DMSO-treated cells (40 g per 10¹² cells) (Figure 5B and C). Moreover, the number of live cells was ~2-fold higher in SR1-treated cultures than in the DMSO-treated control (Figure 5D). We next examined the enucleation rate of these cells and found that SR1 increased the percentage of enucleated erythroid cells by ~2-fold (Figure 5E and F). In addition, we measured the deformation of these cells; SR1-treated cells had a higher deformation index under conditions of 1000 sec⁻¹ shear stress (Figure 5I). Similar results were obtained in UCB-derived erythroid cells (Figure 5C, D, and G–I). These data further support the notion that AHR inhibition promotes erythroid terminal differentiation and function maturation. Furthermore, we showed that H1-derived mature erythroid cells can be obtained by adding AHR antagonists to cell cultures during terminal differentiation.

Discussion

AHR signaling plays profound roles in biological events, particularly in the development and maintenance of HSCs

Figure 2 (Continued) of GPA⁺ cells generated from CD71⁺GPA⁻ cells at D3. (E) Flow cytometry analysis of GPA expression in proerythroblasts at D3. (F) Representative images of MGG-stained cells. Scale bar, 10 μ m. Isolated UCB-derived proerythroblasts were treated with or without SR1, and proteomic analysis of the total cells was performed at D3. (G) Heatmap representing the expression of erythroid-related proteins including skeletal, membrane, and globin proteins; columns represent the indicated replicates of each population, and the colored bar shows row-standardized Z-scores. (H) The expression of β -globin, CD44, and CD47 was analyzed in SR1- or DMSO-treated proerythroblasts by flow cytometry at D3. All values are mean \pm SD, $n = 3$; * $P < 0.05$, ** $P < 0.01$, *** $P < 0.001$.

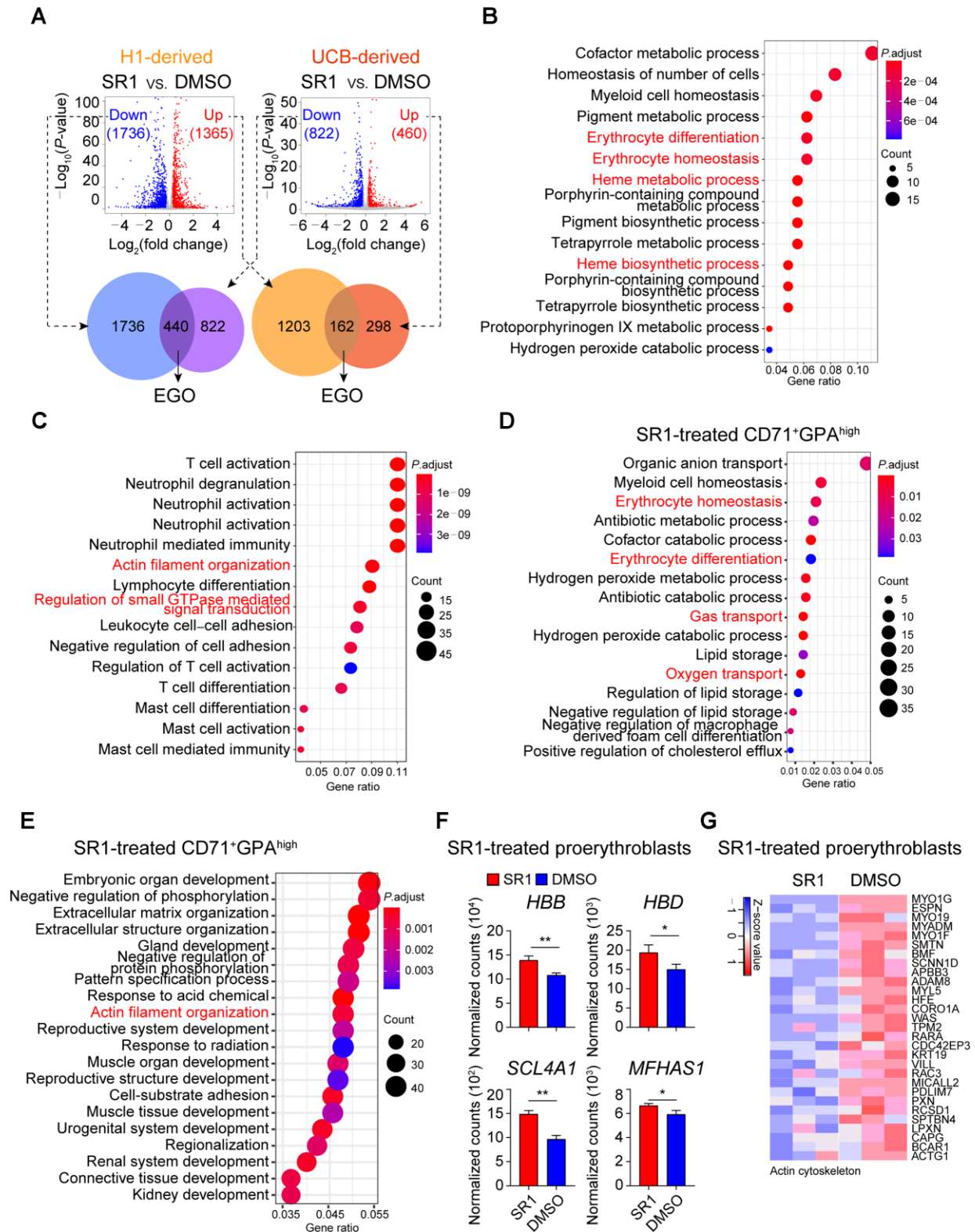


Figure 3 Inhibition of AHR influences heme- and actin-related gene expression during terminal erythroid differentiation. H1- or UCB-derived proerythroblasts were treated with or without SR1 for 3 days; total cells were harvested, and RNA-seq was performed. **(A)** The correlation between RNA expression levels in H1- and UCB-derived proerythroblasts. Detected genes were filtered by P -value < 0.05 and fold change > 1.2 . Differentially expressed RNA transcripts (red, upregulated; blue, downregulated) were assessed for overlap. EGO of genes regulated in

(Boitano et al., 2010; Jackson et al., 2017) and the functional maturation of immune cells (Mascanfroni et al., 2015; Olivier et al., 2016; Angelos et al., 2017; Goudot et al., 2017) and megakaryocytes (Smith et al., 2013), but little is known about how AHR regulates erythroid differentiation. In our present study, through a step-by-step examination of the effects of AHR on the differentiation of erythroid cells, we found that AHR plays an important role in erythroid terminal differentiation.

Many reports show that AHR impacts the expansion and differentiation of HSPCs (Boitano et al., 2010; Lindsey and Papoutsakis, 2012; Jackson et al., 2017) and that AHR antagonists such as SR1 and GNF351 promote the expansion and maintenance of HSPCs (Boitano et al., 2010; Smith et al., 2011; Olivier et al., 2016). In transgenic experimental models, *Ahr*^{-/-} mice showed an increase of HSPCs in bone marrow (Singh et al., 2011), and CFU-E colony formation is increased in *AHR*^{-/-} hESCs (Angelos et al., 2017). Moreover, inhibition of AHR activity increased the differentiation of hematopoietic cells from hPSCs (Angelos et al., 2017). These studies are in agreement with our current study, in which AHR antagonists promoted the development of hESC-derived HSPCs in AGM-S3 co-culture. Particularly, by using SR1 to antagonize AHR signaling at several time points, we observed an increase in the production of erythroid cells from both HSPC-independent and HSPC-dependent pathways during early human hematopoiesis (Figure 1). These data suggest that AHR has an important role in erythropoiesis. We did not observe an increase in the number of CFU-E colonies when HECs (D6 in co-culture) were exposed to SR1 for 3 days (Supplementary Figure S1C). However, hematopoietic colonies containing erythroid cells (mixed colonies and BFU-E) that originated from HPCs at comparatively late stages (D10 in co-culture) were increased, along with the formation of other myeloid colonies (Figure 1D). Furthermore, when co-D14 or UCB-derived CD34⁺ cells were treated with SR1 for 3 days, the percentage of CD71⁺GPA⁺ cells was increased (Figure 1E; Supplementary Figure S1D). These results showed that inhibition of AHR does not directly influence the development of erythroid cells from multipotent hematopoietic progenitors, but might affect the late erythroblast differentiation stage.

Commitment to an erythroid lineage is typically marked by the appearance of BFU-E cells, defined as CD34⁺CD71^{low}GPA⁻CD36⁻CD123⁻ (Li et al., 2014). In our current study, we found that SR1 mostly exerts its effect at the BFU-E stage to promote CFU-E production and the further maturation of erythroblasts. Activation of AHR can generate erythroid progenitors from hiPSC-derived erythroid-

megakaryocyte precursors (Smith et al., 2013). Consistent with this report, we observed a moderate decrease in the production of erythroid cells from UCB-CD34⁺ cells when SR1 was continuously added to the culture (Supplementary Figure S1E). However, when SR1 treatment was pulsed within 3 days, purified UCB-BFU-E cells produced more CFU-E colonies in semisolid culture and produced CD71⁺GPA⁺ cells in suspension culture (Figure 2A–C), and UCB-CFU-E cells produced more CD71⁺GPA⁺ cells as well (Figure 2D). Furthermore, antagonizing AHR accelerated terminal differentiation of proerythroblasts (Figure 2E). These effects were prevented by adding TCDD to the culture, showing that SR1 directly targets AHR signaling to promote terminal differentiation of erythroblasts. We gained similar results from hESC-derived early erythroblasts and co-D14 CD34⁺ cell-derived proerythroblasts. Thus, our findings show that the role of AHR in erythroid differentiation is dependent upon the stage of erythroid differentiation. Initially, antagonizing AHR signaling promotes the generation of hPSC-derived HSPCs, resulting in a parallel increased production of erythroid cells. While at early erythroid-megakaryocyte precursor stage, AHR signaling helps generate more erythroid cells before commitment to the erythroid lineage, it has no effect after that. Once committed to erythroid lineage, antagonism of AHR signaling enhances the terminal differentiation of erythroblasts, irrespective of the origin of these cells, suggesting that suppression of AHR signaling conveys a regulatory mechanism on erythroid terminal differentiation and functional maturation, which is common to all erythroblasts.

Through transcriptomic analysis by RNA-seq, we found that SR1 upregulated the expression of 162 overlapping genes in both UCB- and hESC-derived proerythroblasts. These genes were highly enriched in erythroid maturation processes, such as erythroid differentiation and homeostasis, as well as heme metabolic processes. This finding demonstrated that antagonizing AHR signaling comprehensively promotes the terminal differentiation and maturation of erythroblasts (Figure 3). Interestingly, RNA-seq results showed that SR1 downregulated the expression of genes highly associated with AHR (Supplementary Figure S4A). Among these genes, the expression of *CYP1B1* (a gene that is downstream of AHR), but not *CYP1A1*, was downregulated. Since previous reports showed that *CYP1A1* is predominantly expressed in blood cells (Villa et al., 2017; Lv et al., 2018), our finding might highlight a novel role for *CYP1B1* in AHR-mediated oxidative stress during erythroid cell differentiation.

Figure 3 (Continued) both H1- and UCB-derived cells was performed. (B and C) EGO analysis of the 162 co-upregulated (B) and 440 co-downregulated (C) genes using the clusterProfiler R package: each symbol represents a GO term (noted in the plot); the color indicates the adjusted *P*-value. UCB-derived erythroid cells were exposed to SR1 or DMSO for 3 days, and treated proerythroblasts and CD71⁺GPA^{high} cells were sorted for RNA-seq analysis at D10. (D and E) EGO analysis showed upregulated (D) and downregulated (E) genes in SR1-treated CD71⁺GPA^{high} cells. (F) The expression of *HBB*, *HBD*, *SCL4A1*, and *MFHAS1* in treated proerythroblasts from RNA-seq data. (G) Heatmap analysis of actin-cytoskeleton-related genes in these cells; columns represent the indicated replicates of each population; the color bar shows row-standardized Z-scores.

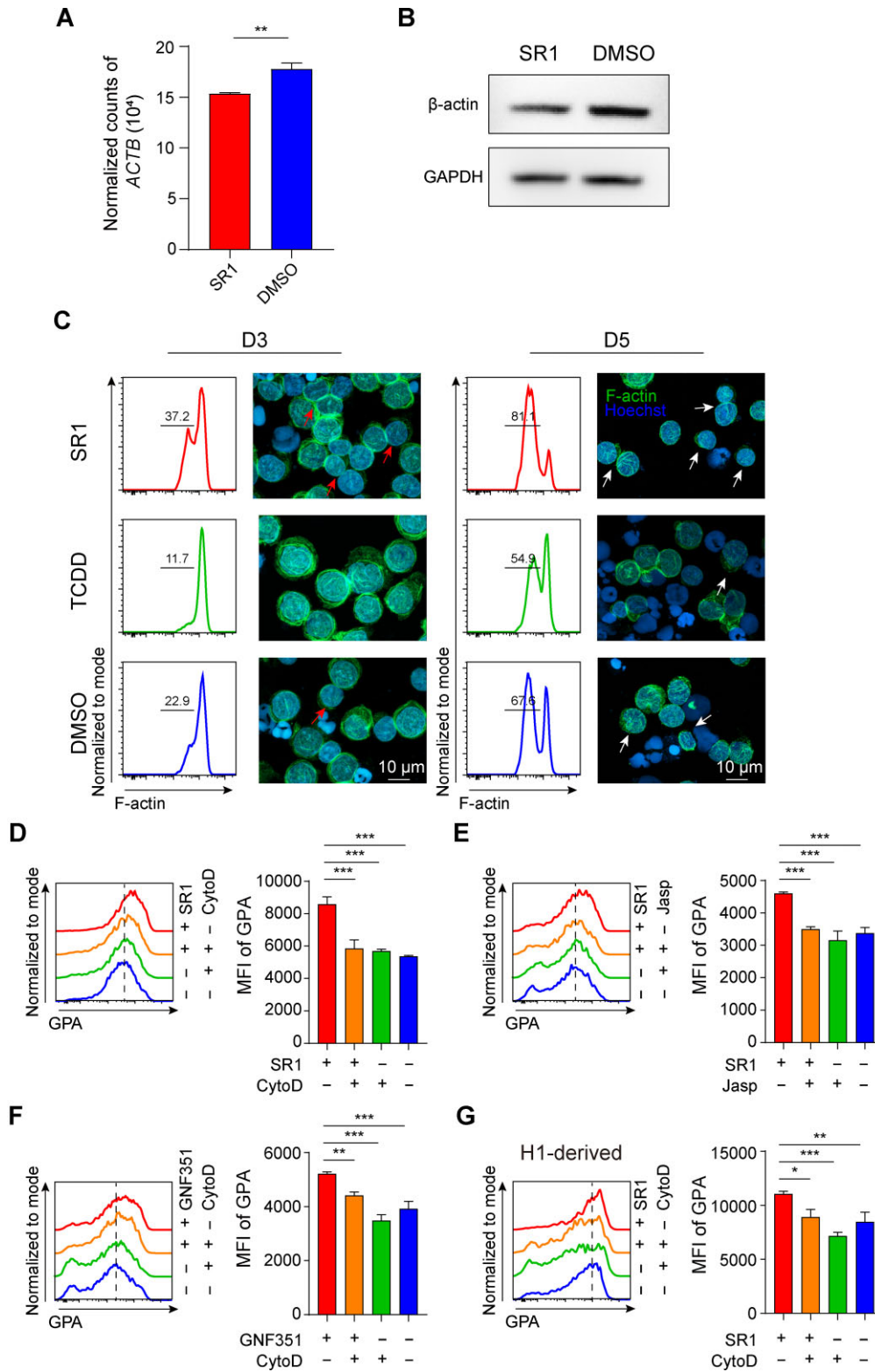


Figure 4 Disrupting F-actin assembling can block the function of AHR antagonists on erythroid terminal differentiation. **(A and B)** The expression of β-actin in SR1-treated UCB-derived proerythroblasts was detected by RNA-seq **(A)** and western blotting analysis **(B)** at D3. **(C)** F-actin was detected in UCB-derived proerythroblasts continuously treated with SR1, TCDD, or DMSO at D3 and D5. The proportion of F-actin was analyzed by flow cytometry, and the structure of F-actin was observed by IF staining; phalloidin (green staining) represents F-actin,

Further analysis revealed that SR1 treatment downregulated the expression of 440 genes common to both UCB- and hESC-derived proerythroblasts. In particular, actin cytoskeleton-related genes were highly enriched. Our findings suggest that the function of AHR antagonism in promoting erythroid terminal differentiation is related to modulation of actin activity. Actin is an erythroid cytoskeleton protein that has an essential role in normal erythropoiesis (Nigra et al., 2020), and thus our finding may be important in better understanding the mechanism by which AHR regulation promotes the terminal maturation of erythroblasts. During terminal erythroid differentiation, the expression of actin peaks in proerythroblasts and then decreases in subsequent differentiation stages (Wickrema et al., 1994; Chen et al., 2009; Nowak et al., 2017). In our experiments, we found that SR1-treated cells had lower F-actin expression than TCDD-treated cells, in which F-actin expression did not alter at D3 (Figure 4C). Treatment with SR1 accelerated F-actin remodeling, but lots of TCDD-treated cells remained in a ring structure. This finding is in agreement with reports showing that during erythroid cell maturation, F-actin rearranges and forms a contractile ring between the extruding nucleus and the incipient reticulocyte; this process is essential to enucleation (Nigra et al., 2020). Moreover, the effect of AHR antagonists on terminal erythroid differentiation was reversed by actin-disrupting drugs (Figure 4D–G). Taken together, our results demonstrate that there is a correlation between AHR and F-actin during terminal erythroid differentiation.

We, and other groups, have reported that a large number of functionally mature erythrocytes could be generated from hESCs *in vitro* (Lu et al., 2008; Ma et al., 2008; Mao et al., 2016), but it is still difficult to undergo enucleation for these cells. In our experiments on mature hESC-derived erythrocytes, inhibition of AHR signaling also promoted terminal erythroid differentiation, with cells showing a more mature morphology and better deformability. Moreover, SR1 treatment resulted in a 2-fold increase in the number of enucleated erythrocytes (Figure 5). This positive effect of AHR antagonists on erythropoiesis, coupled with SR1-facilitated production of hESC-derived HSPCs, points to a novel approach for the large-scale production of mature erythroid cells from hPSCs.

In summary, our study shows that antagonizing AHR signaling accelerates erythroid terminal differentiation. Our exploration of the mechanism that underlies this effect suggests that inhibition of the AHR pathway induces an oxidative stress response in proerythroblasts and accelerates the actin-mediated rearrangement of the cytoskeleton. Future studies aiming at better understanding the regulation of AHR signaling during terminal

erythroid differentiation might uncover further molecular mechanisms. Our study also provides a novel approach for the large-scale production of hPSC-derived mature erythrocytes.

Materials and methods

Maintenance of hESCs

H1 hESCs were provided by Prof. Tao Cheng and maintained on Matrigel-coated plates in mTeSR medium (Stem Cell Technologies) as described previously (Mao et al., 2016; Zhou et al., 2019). Cells were dissociated into clumps using ReLeSR (Stem Cell Technologies).

Differentiation of hESCs into HSPCs

hESCs (5×10^4) were plated on irradiated AGM-S3 (13.5 Gy). Cells were induced into HSPCs after 3-day maintenance culturing as described previously (Mao et al., 2016; Zhou et al., 2019). SR1 (750 nM), TCDD (10 nM) (Angelos et al., 2017), or DMSO (used as vehicle control) was added at co-D6.

Differentiation of HSPCs into erythroid cells

To generate erythroid cells from co-cultured cells, co-D12 or co-D14 CD34⁺ cells were isolated using a human CD34 positive selection kit (Stem Cell Technologies). CD34⁺ cells (1×10^5 /ml) were suspended in serum-free expansion medium II (Stem Cell Technologies) with 50 ng/ml stem cell factor (PeproTech), thrombopoietin (PeproTech), Fms-related tyrosine kinase 3 ligand (PeproTech), and 0.5% penicillin/streptomycin (Invitrogen). After 3 days in HSPC expansion culture, the cells were cultured using a three-phase liquid culture system (described in Supplementary Methods). To generate UCB-derived erythroid cells, CD34⁺ cells were sorted using the same method described above, and then the cells were cultured in a three-phase liquid culture system.

Hematopoietic colony assay

Cells were cultured on colony assay medium described previously (Ma et al., 2008; Mao et al., 2016; Zhou et al., 2019; Dong et al., 2020). Briefly, cells were cultured on methylcellulose supplemented with cytokines and 0.5% penicillin/streptomycin (Invitrogen). BFU-E, CFU-E, GEMM, and G/M/GM colonies were assessed after 12–14 days.

Flow cytometry and cell sorting

Co-cultured cells were harvested by 0.25% trypsin–ethylenediaminetetraacetic acid (Invitrogen) as described previously (Zhou et al., 2019). Cells were incubated with

Figure 4 (Continued) and nuclei are stained blue; the red arrow indicates actin remodeling, and the white arrow indicates polarized actin; scale bar, 20 μ m. (D and E) UCB-derived proerythroblasts were treated with or without the actin-disrupting drug, CytoD or jasplakinolide (Jasp), under SR1- or DMSO-treated conditions. GPA expression in CytoD-treated (D) and Jasp-treated (E) cells was analyzed by flow cytometry at D3, and the mean fluorescence intensity (MFI) of GPA in these cells was calculated. (F) UCB-derived CD71⁺ GPA^{low} cells were treated with or without CytoD under GNF351- or DMSO-treated conditions. GPA expression was analyzed by flow cytometry and the MFI of GPA was calculated at D3. (G) H1-derived proerythroblasts were treated with or without CytoD under SR1- or DMSO-treated conditions. GPA expression was analyzed by flow cytometry and the MFI of GPA was calculated at D3. All values are mean \pm SD, $n = 3$; * $P < 0.05$, ** $P < 0.01$, *** $P < 0.001$.

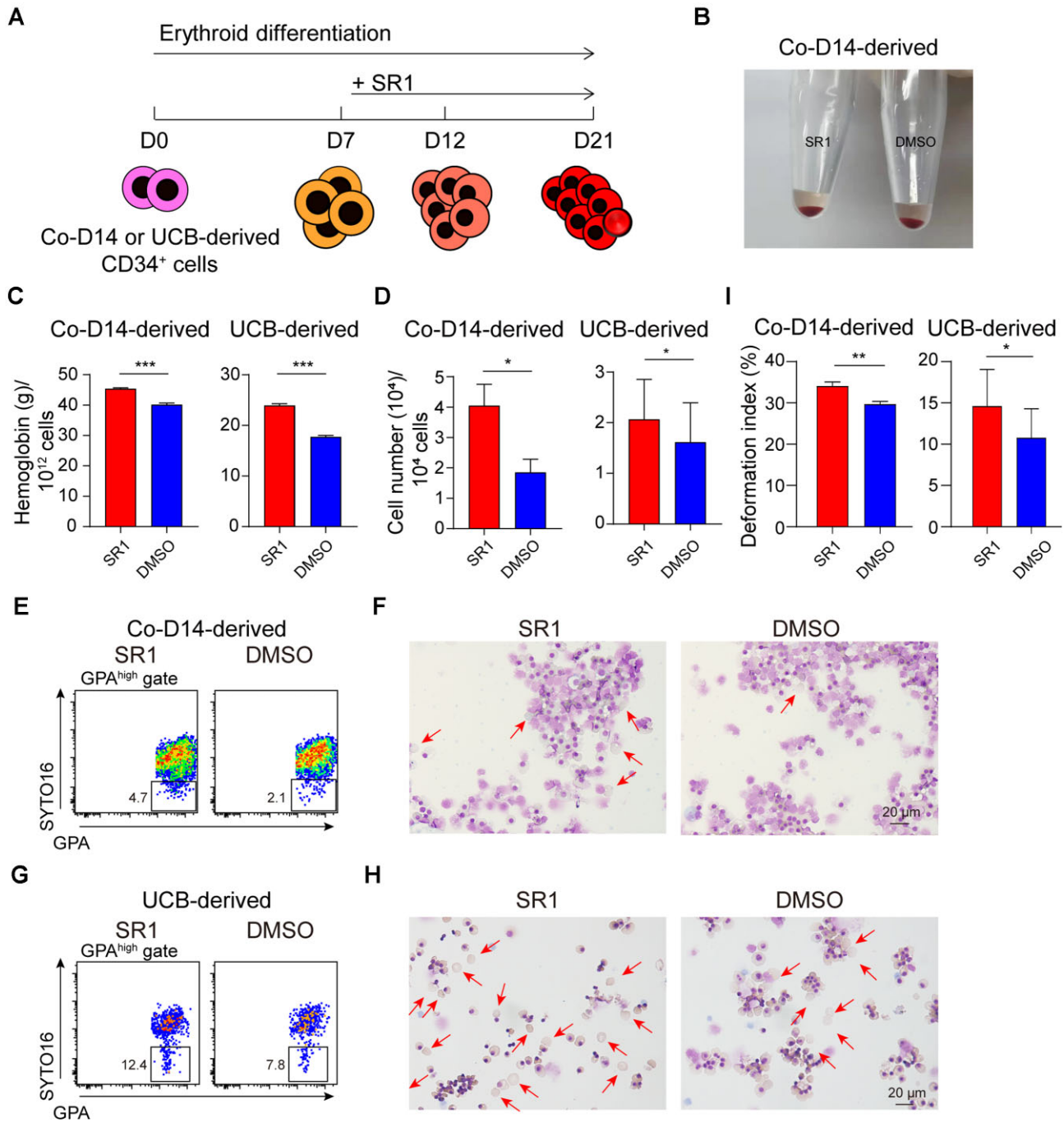


Figure 5 SR1 benefits the functional maturation of human erythroid cells. **(A)** A schematic of the strategy used to produce functional maturation of human erythroid cells. SR1 was added on D7, and erythroid cells were collected at D21. **(B)** Images show co-D14-derived erythroid cells harvested at D21. **(C and D)** Hemoglobin concentration **(C)** and the number of live cells **(D)** of co-D14- and UCB-derived erythroid cells were calculated at D21. **(E–H)** The enucleation rate of co-D14- **(E)** and UCB-derived **(G)** erythroid cells was analyzed by flow cytometry, and the morphology of co-D14- **(F)** and UCB-derived **(H)** cells was observed by MGG staining at D21; representative images of erythroid cells are shown. The red arrow indicates enucleated erythrocytes; scale bar, 20 μ m. **(I)** the deformability of co-D14- and UCB-derived erythroid cells was detected at D21. All values are mean \pm SD, $n = 3$; * $P < 0.05$, ** $P < 0.01$, *** $P < 0.001$.

anti-human Fc block on ice for 20 min and then incubated with antibodies for 30 min. Flow cytometry was performed by using an FACS Canto II system (BD Biosciences) and cells were sorted by using an FACS Cytometer System (FACSJazz, BD). The antibodies used are presented in Supplementary Table S1. Data were analyzed using FlowJo software (v.10.0.8).

Morphological observation and immunofluorescence staining analysis

Harvested cells were centrifuged on glass slides by a cell cytospin machine (Cytospin 4, Thermo Fisher Scientific). Morphology and membrane proteins were observed by May-Grunwald Giemsa (MGG) and immunofluorescence (IF) staining, respectively, as described previously (Mao et al., 2016; Zhou et al., 2019). The antibodies for IF staining are presented in Supplementary Table S1.

RNA-seq and data analysis

UCB-derived and hESC-derived proerythroblasts (CD71⁺GPA^{low}), which were treated with SR1 or DMSO, were collected at D3. Besides, UCB-derived erythroid cells were treated with SR1 or DMSO at D7, and the treated proerythroblasts and CD71⁺GPA^{high} cells were sorted at D10. Samples were dealt with Trizol (Invitrogen). A DNA library was generated and sequenced by Novogene Co., Ltd. All fastq sequences were aligned to the hg38 human genome using Hisat2 software. Normalized data and differential expression gene analyses were performed using DESeq2. EGO analysis, GSEA, and heatmap analysis were performed on raw data as described previously (Dong et al., 2020). The sequence data reported in this study were archived in the Sequence Read Archive with the accession number PRJNA724809.

F-actin staining assay

Erythroid cells were harvested and washed three times with phosphate-buffered saline (PBS). Cells were fixed with 4% paraformaldehyde for 10 min at room temperature, followed by permeabilization in 0.1% Triton X-100 for 2 min at room temperature. After washing, cells were blocked with 1% bovine serum albumin (BSA) for 20 min at room temperature, and then washed three times with PBS. Subsequently, fluorescent fluorescein-isothiocyanate-conjugated phalloidin (MedChemExpress) diluted in 1% BSA (5 μ g/ml) was added and incubated for 30 min at 37°C. After nuclear staining with Hoechst 33342 (Invitrogen), cells were centrifuged on glass slides. Images were acquired using a ZEISS LSM900 Airyscan microscope.

Deformability measurements

Erythroid cells (1×10^6) were resuspended in 10 μ l PBS and added to 1 ml polyvinylpyrrolidone solution. The mixture was transferred to ektacytometry (LBY-BY). Deformability was assessed using the elongation index measured by the tester under shear-rate conditions of 1000 sec⁻¹.

Statistical analysis

All data are shown as mean \pm SD from three independent experiments. Statistical significance was evaluated using Student's *t*-test (when two groups were analyzed) or one-way analysis of variance with Tukey's multiple testing corrections as appropriate (for three or more groups). A *P*-value <0.05 was considered significant.

Supplementary material

Supplementary material is available at *Journal of Molecular Cell Biology* online.

Acknowledgements

We thank Prof. Tao Cheng at State Key Laboratory of Experimental Hematology, Institute of Hematology and Blood Diseases Hospital, CAMS & PIMC, for generously providing the H1 line. We also thank Prof. Duonan Yu for precious suggestions on this work.

Funding

This work was supported by the National Basic Research Program (973 Program; 2015CB964902), the National Natural Science Foundation of China (H81170466 and H81370597), the CAMS Initiatives for Innovative Medicine (2016-I2M-1-018, 2019-I2M-1-006, and 2017-I2M-2005) to F.M., and the National Natural Science Foundation of China Youth Fund (82000119) to Yonggang Zhang.

Conflict of interest: none declared.

Author contributions: Y.C. performed research and analyzed data. Y.D. performed RNA-seq and proteomics data analysis. X. Lu, W.L., Yimeng Zhang, B.M., X.P., X. Li, Ya Zhang, Q.A., F.X., Y.X., X.C., M.L., Q.Z., and Yonggang Zhang performed some of the experiments. Y.Y. and R.F. provided umbilical cord blood. Y.C. and F.M. designed the project, discussed the data, and wrote the manuscript. F.M. funded the research project and approved the final manuscript.

References

- An, X., Schulz, V.P., Li, J., et al. (2014). Global transcriptome analyses of human and murine terminal erythroid differentiation. *Blood* 123, 3466–3477.
- Angelos, M.G., and Kaufman, D.S. (2018). Advances in the role of the aryl hydrocarbon receptor to regulate early hematopoietic development. *Curr. Opin. Hematol.* 25, 273–278.
- Angelos, M.G., Ruh, P.N., Webber, B.R., et al. (2017). Aryl hydrocarbon receptor inhibition promotes hematolymphoid development from human pluripotent stem cells. *Blood* 129, 3428–3439.
- Belair, C.D., Peterson, R.E., and Heideman, W. (2001). Disruption of erythropoiesis by dioxin in the zebrafish. *Dev. Dyn.* 222, 581–594.
- Bennett, J.A., Singh, K.P., Welle, S.L., et al. (2018). Conditional deletion of Ahr alters gene expression profiles in hematopoietic stem cells. *PLoS One* 13, e0206407.
- Boitano, A.E., Wang, J., Romeo, R., et al. (2010). Aryl hydrocarbon receptor antagonists promote the expansion of human hematopoietic stem cells. *Science* 329, 1345–1348.

- Carney, S.A., Prasad, A.L., Heideman, W., et al. (2006). Understanding dioxin developmental toxicity using the zebrafish model. *Birth Defects Res. A Clin. Mol. Teratol.* 76, 7–18.
- Carvajal-Gonzalez, J.M., Mulero-Navarro, S., Roman, A.C., et al. (2009). The dioxin receptor regulates the constitutive expression of the vav3 proto-oncogene and modulates cell shape and adhesion. *Mol. Biol. Cell* 20, 1715–1727.
- Chen, K., Liu, J., Heck, S., et al. (2009). Resolving the distinct stages in erythroid differentiation based on dynamic changes in membrane protein expression during erythropoiesis. *Proc. Natl Acad. Sci. USA* 106, 17413–17418.
- Dong, Y., Bai, J., Zhang, Y., et al. (2020). Alpha lipoic acid promotes development of hematopoietic progenitors derived from human embryonic stem cells by antagonizing ROS signals. *J. Leukocyte Biol.* 108, 1711–1725.
- Furue, M., Hashimoto-Hachiya, A., and Tsuji, G. (2018). Antioxidative phytochemicals accelerate epidermal terminal differentiation via the AHR–OVOL1 pathway: implications for atopic dermatitis. *Acta Derm. Venereol.* 98, 918–923.
- Goudot, C., Coillard, A., Villani, A.-C., et al. (2017). Aryl hydrocarbon receptor controls monocyte differentiation into dendritic cells versus macrophages. *Immunity* 47, 582–596.e6.
- Guarnieri, T., Abruzzo, P.M., and Bolotta, A. (2020). More than a cell biosensor: aryl hydrocarbon receptor at the intersection of physiology and inflammation. *Am. J. Physiol. Cell Physiol.* 318, C1078–C1082.
- Hattangadi, S.M., Wong, P., Zhang, L., et al. (2011). From stem cell to red cell: regulation of erythropoiesis at multiple levels by multiple proteins, RNAs, and chromatin modifications. *Blood* 118, 6258–6268.
- Jackson, C.S., Durandt, C., Janse van Rensburg, I., et al. (2017). Targeting the aryl hydrocarbon receptor nuclear translocator complex with DMOG and Stemregenin 1 improves primitive hematopoietic stem cell expansion. *Stem Cell Res.* 21, 124–131.
- Juricek, L., Carcaud, J., Pelhaitre, A., et al. (2017). AhR-deficiency as a cause of demyelinating disease and inflammation. *Sci. Rep.* 7, 9794.
- Juricek, L., and Coumoul, X. (2018). The aryl hydrocarbon receptor and the nervous system. *Int. J. Mol. Sci.* 19, 2504.
- Leung, A., Zulick, E., Skvir, N., et al. (2018). Notch and aryl hydrocarbon receptor signaling impact definitive hematopoiesis from human pluripotent stem cells. *Stem Cells* 36, 1004–1019.
- Li, J., Bhattacharya, S., Zhou, J., et al. (2017a). Aryl hydrocarbon receptor activation suppresses EBF1 and PAX5 and impairs human B lymphopoiesis. *J. Immunol.* 199, 3504–3515.
- Li, J., Hale, J., Bhagia, P., et al. (2014). Isolation and transcriptome analyses of human erythroid progenitors: BFU-E and CFU-E. *Blood* 124, 3636–3645.
- Li, X., Mei, Y., Yan, B., et al. (2017b). Histone deacetylase 6 regulates cytokinesis and erythrocyte enucleation through deacetylation of formin protein mDia2. *Haematologica* 102, 984–994.
- Lindsey, S., and Papoutsakis, E.T. (2011). The aryl hydrocarbon receptor (AHR) transcription factor regulates megakaryocytic polyploidization. *Br. J. Haematol.* 152, 469–484.
- Lindsey, S., and Papoutsakis, E.T. (2012). The evolving role of the aryl hydrocarbon receptor (AHR) in the normophysiology of hematopoiesis. *Stem Cell Rev. Rep.* 8, 1223–1235.
- Lu, S.J., Feng, Q., Park, J.S., et al. (2008). Biologic properties and enucleation of red blood cells from human embryonic stem cells. *Blood* 112, 4475–4484.
- Ludwig, L.S., Lareau, C.A., Bao, E.L., et al. (2019). Transcriptional states and chromatin accessibility underlying human erythropoiesis. *Cell Rep.* 27, 3228–3240.e7.
- Lv, Q., Shi, C., Qiao, S., et al. (2018). Alpinetin exerts anti-colitis efficacy by activating AHR, regulating miR-302/DNMT-1/CREB signals, and therefore promoting Treg differentiation. *Cell Death Dis.* 9, 890.
- Ma, F., Ebihara, Y., Umeda, K., et al. (2008). Generation of functional erythrocytes from human embryonic stem cell-derived definitive hematopoiesis. *Proc. Natl Acad. Sci. USA* 105, 13087–13092.
- Mao, B., Huang, S., Lu, X., et al. (2016). Early development of definitive erythroblasts from human pluripotent stem cells defined by expression of glycophorin A/CD235a, CD34, and CD36. *Stem Cell Rep.* 7, 869–883.
- Mascanfroni, I.D., Takenaka, M.C., Yeste, A., et al. (2015). Metabolic control of type 1 regulatory T cell differentiation by AHR and HIF1- α . *Nat. Med.* 21, 638–646.
- Merches, K., Schiavi, A., Weighardt, H., et al. (2020). AHR signaling dampens inflammatory signature in neonatal skin $\gamma\delta$ T cells. *Int. J. Mol. Sci.* 21, 2249.
- Murai, M., Tsuji, G., Hashimoto-Hachiya, A., et al. (2018). An endogenous tryptophan photo-product, FICZ, is potentially involved in photo-aging by reducing TGF- β -regulated collagen homeostasis. *J. Dermatol. Sci.* 89, 19–26.
- Murray, I.A., Patterson, A.D., and Perdew, G.H. (2014). Aryl hydrocarbon receptor ligands in cancer: friend and foe. *Nat. Rev. Cancer* 14, 801–814.
- Neavin, D.R., Liu, D., Ray, B., et al. (2018). The role of the aryl hydrocarbon receptor (AHR) in immune and inflammatory diseases. *Int. J. Mol. Sci.* 19, 3851.
- Nebert, D.W. (2017). Aryl hydrocarbon receptor (AHR): ‘pioneer member’ of the basic-helix/loop/helix per–Arnt–sim (bHLH/PAS) family of ‘sensors’ of foreign and endogenous signals. *Prog. Lipid Res.* 67, 38–57.
- Nigra, A.D., Casale, C.H., and Santander, V.S. (2020). Human erythrocytes: cytoskeleton and its origin. *Cell. Mol. Life Sci.* 77, 1681–1694.
- Nowak, R.B., Papoin, J., Gokhin, D.S., et al. (2017). Tropomodulin 1 controls erythroblast enucleation via regulation of F-actin in the enucleosome. *Blood* 130, 1144–1155.
- Olivier, E.N., Marenah, L., McCahill, A., et al. (2016). High-efficiency serum-free feeder-free erythroid differentiation of human pluripotent stem cells using small molecules. *Stem Cells Transl. Med.* 5, 1394–1405.
- Reyes-Hernandez, O.D., Mejia-Garcia, A., Sanchez-Ocampo, E.M., et al. (2009). Aromatic hydrocarbons upregulate glyceraldehyde-3-phosphate dehydrogenase and induce changes in actin cytoskeleton. Role of the aryl hydrocarbon receptor (AhR). *Toxicology* 266, 30–37.
- Sakamoto, M.K., Mima, S., Kihara, T., et al. (2004). Sequential morphological changes of erythrocyte apoptosis in *Xenopus* larvae exposed to 2,3,7,8-tetrachlorodibenzo-p-dioxin (TCDD). *Anat. Rec. A Discov. Mol. Cell. Evol. Biol.* 279, 652–663.
- Scoville, S.D., Nalin, A.P., Chen, L., et al. (2018). Human AML activates the aryl hydrocarbon receptor pathway to impair NK cell development and function. *Blood* 132, 1792–1804.
- Sherr, D.H., and Monti, S. (2013). The role of the aryl hydrocarbon receptor in normal and malignant B cell development. *Semin. Immunopathol.* 35, 705–716.
- Shinde, R., Hezaveh, K., Halaby, M.J., et al. (2018). Apoptotic cell-induced AHR activity is required for immunological tolerance and suppression of systemic lupus erythematosus in mice and humans. *Nat. Immunol.* 19, 571–582.
- Singh, K.P., Garrett, R.W., Casado, F.L., et al. (2011). Aryl hydrocarbon receptor-null allele mice have hematopoietic stem/progenitor cells with abnormal characteristics and functions. *Stem Cells Dev.* 20, 769–784.
- Smith, B.W., Rozelle, S.S., Leung, A., et al. (2013). The aryl hydrocarbon receptor directs hematopoietic progenitor cell expansion and differentiation. *Blood* 122, 376–385.
- Smith, K.J., Murray, I.A., Tanos, R., et al. (2011). Identification of a high-affinity ligand that exhibits complete aryl hydrocarbon receptor antagonism. *J. Pharmacol. Exp. Ther.* 338, 318–327.
- Strassel, C., Brouard, N., Mallo, L., et al. (2016). Aryl hydrocarbon receptor-dependent enrichment of a megakaryocytic precursor with a high potential to produce platelets. *Blood* 127, 2231–2240.
- Ubukawa, K., Goto, T., Asanuma, K., et al. (2020). Cdc42 regulates cell polarization and contractile actomyosin rings during terminal differentiation of human erythroblasts. *Sci. Rep.* 10, 11806.
- Unnisa, Z., Singh, K.P., Henry, E.C., et al. (2016). Aryl hydrocarbon receptor deficiency in an exon 3 deletion mouse model promotes hematopoietic

- stem cell proliferation and impacts endosteal niche cells. *Stem Cells Int.* 2016, 4536187.
- Uras, I.Z., Scheicher, R.M., Kollmann, K., et al. (2017). Cdk6 contributes to cytoskeletal stability in erythroid cells. *Haematologica* 102, 995–1005.
- Villa, M., Gialitakis, M., Tolaini, M., et al. (2017). Aryl hydrocarbon receptor is required for optimal B-cell proliferation. *EMBO J.* 36, 116–128.
- Wickrema, A., Koury, S.T., Dai, C.H., et al. (1994). Changes in cytoskeletal proteins and their mRNAs during maturation of human erythroid progenitor cells. *J. Cell. Physiol.* 160, 417–426.
- Zhou, Y., Zhang, Y., Chen, B., et al. (2019). Overexpression of GATA2 enhances development and maintenance of human embryonic stem cell-derived hematopoietic stem cell-like progenitors. *Stem Cell Rep.* 13, 31–47.